Nano-structure zinc and cadmium azide and thiocyanate complexes: Synthesis, characterization, thermal, antimicrobial and DNA interaction

S. A. Musavi[1], M. Montazerozohori[1*], M. Nasr-Esfahani[1], R. Naghiha[2], M. Montazer Zohour[3]

[1]Department of Chemistry, Yasouj University, Yasouj 75918-74831, Iran.
[2]Department of Animal Sciences, Faculty of Agriculture, Yasouj University, Yasouj, Iran.
[3]Genetics of Non-Communicable Disease Research Center, Zahedan University of Medical Sciences, Zahedan, Iran

Three nano-structure azide and thiocyanate zinc and cadmium complexes of a Schiff base ligand were prepared and characterized by conductivity measurements, elemental analysis, IR, UV–Visible, ^1H and ^{13}C NMR Spectroscopy and thermo-gravimetric studies. Detectable changes in the spectral data suggested coordination of ligand to zinc and cadmium ions. The proposed formula structure of the complexes was found to be MLX_2. Nano-size structure of the complexes was confirmed by transmission electron microscopy (TEM). The average particle sizes of the complexes were found to be in the range of 25.32 - 85.11 nm. Thermal analyses of the complexes was carried out. The thermal curves showed that zinc thiocyanate was decomposed via six thermal steps while cadmium azide and thiocyanate complexes were thermally degraded via three steps. Moreover some activation thermodynamic parameters such as the activation energy, enthalpy, entropy and Gibbs-free energy of activation and the Arrhenius constant were calculated based on TG/DTG curves. The antimicrobial behavior with respect to bacteria of *Escherichia coli*, *Pseudomonas aereuguinosa*, *Staphylococcus aureus*, *Bacillus subtillis* and a fungus (*Candida albicans*) was investigated. $ZnL(NCS)_2$ was found to have more antifungal activity against *Candida albicans* than others. Finally, the interaction of the complexes with DNA ($pMalC_2X$ DNA of *Escherichia coli*) was checked to investigate their cleavage potential.

Keywords: Schiff base, antimicrobial, thermal, transmission electron microscopy, nano-structure.

INTRODUCTION

Metal complexes including a central metal atom or ion is surrounded by a series of ligands and play an important role from an inorganic chemistry point of view especially for elements of the d-block. Recently various organic ligands containing N, O and S donor atoms have been used for preparation of metal complexes. Schiff base ligands have an important role in the development of the field of coordination chemistry [1-7]. Such ligands and their complexes are of interest due to their catalytic activity in some reactions such as epoxidation, carbonylation, oxidation and carbon–carbon coupling reactions. The other reason of importance of these types of compounds is their biological activity in containing anti-inflammatory activity, antibiotic activity, antimicrobial activity and antitumor activity. The DNA binding or cleavage interaction of Schiff base complexes is the other major application of these compounds in the field of biochemistry [8-19]. Nowadays the synthesis of nanostructure coordination compounds is of interest for many researchers. This interest may be due to specific properties as compared with bulk compounds. The notable characteristics of nano-structure compounds originate from their large surface area with respect to bulk materials. Various methods are used for the preparation of nano-structure compounds and synthesis under ultrasonic conditions is one of the common techniques.

As part of our continued work in the synthesis of metal complexes of Schiff base ligands [20-23], herein we report on the synthesis and characterization of three nano structure zinc and cadmium azide and thiocyanate complexes of a Schiff base ligand (L) with the general formula MLX_2 whereas X= SCN^- and N_3^-. These compounds have been characterized by physical and spectral data including elemental analysis, conductance data, FT-IR, UV-Vis, ^1H and ^{13}C-NMR spectroscopy. TEM images were used to confirm the nano-size structure of all complexes. Furthermore, the DNA interaction, antimicrobial activities and thermal behavior of the complexes were investigated.

EXPERIMENTAL
MATERIALS AND METHODS

All solvents used in the synthesis and analysis of N'-(2-Amino-ethyl)-ethane-1,2-diamineand 4-nitro-benzaldehyde were purchased from Aldrich and Merck and used without any further purification. In biological tests, Nutrient agar (Merck, Germany)

---

was used to prepare nutrient plates while Mueller Hinton broth (Scharlab) was used for the liquid culture media. The *Escherichia coli*(ATCC 25922), *Pseudomonas aereuguinosa* (ATCC 9027), *Staphylococcus aureus* (ATCC 6538) and *Bacillus subtillis* (ATCC 6633) were used for antibacterial and *Candidalbicans* for the antifungal investigations. The FT-IR spectra were recorded on the JASCO-680 model in the range of 400-4000 cm^{-1} using KBr discs. Elemental analyses data (C, H and N) were obtained by a CHNS-932(leco) elemental analyzer. UV-Visible spectra were recorded using a JASCO-V570 spectrometer of DMF solution in the 200-800 nm range. ^{1}H and ^{13}C NMR spectra were recorded using a Brucker DPX FT-NMR spectrometer at 400 MHz in DMSO-d$_6$ using TMS as the internal standard. Molar conductance data of the ligand and their metal complexes were measured in DMF (1.0×10^{-3} M) at room temperature using a SelectaLab ECW 312 microprocessor conductivity meter. The ultrasonic instrument used in the synthesis process was an ultrasonic bath (Tecno-Gasz SPA, Parma, Italy) with a frequency of 40 kHz and 130 W. The melting points (ºC) of the complexes were recorded on a Kruss instrument. The TG/DTG curves were obtained from a Diamond TGA PerkinElmer 60 Hz. The transmission electron microscopy (TEM) images were recorded on a Zeiss EM900 transmission electron microscope with an accelerating voltage of 80 kV.

Synthesis of Schiff base ligand

The Schiff base of (E)-N-(4-nitrobenzylidene)-2-(2-(4-nitrophenyl)imidazolidine-1-yl) ethanamine(L) was synthesized by a condensation reaction between 2 mmol of 4-nitro-benzaldehyde and 1 mmol of N'-(2-Amino-ethyl)-ethane-1,2-diamine in 30 mL methanolic solution according to our previous report[23]. After 2h, the ligand was filtered as cream precipitate and washed twice with cooled methanol and then dried on the vacuum apparatus. The characteristic data of IR, UV-Visible, ^{1}HNMR and ^{13}CNMR have been tabulated as table 1, 2 and 3.

Preparation of nano-structure MLX$_2$ complexes (M= Zn(II) and Cd(II)and X= SCN$^-$ and N$_3^-$)

At first, ethanolic solution of zinc and cadmium thiocyanate or azide were prepared by a reaction between zinc or cadmium nitrate (1 mmol) and potassium thiocyante or sodium azide (2 mmol) in 20 mL ethanol and then filtration. For preparation of the nano-structure complexes, 15 mL of fresh ethanolic solution of MX$_2$ was placed in an ultrasonic condition at a temperature of 60 °C. Into this solution, 15 mL of a methanolic solution of the Schiff base ligand was added drop wise in a 1:1 molar ratio. After 1 h, the precipitate was filtered off, washed with cooled ethanol and then dried in the vacuum apparatus.

Antimicrobial activity assay procedure

To investigate the activity of the titled compounds as antibacterial and antifungal agents *in vitro* four bacteria and a fungus species were selected. The disk diffusion technique was employed for biological studies on *Escherichia coli and Pseudomonas aeruginosa as* Gram negative*; Staphylococcus aureus* and *Bacillus subtillis* as Gram positive and *Candid albicans* as a fungus. The stock solution of each compound was prepared in DMSO solvent (500 µg/mL). Muller Hinton broth was used for preparation of the basal media for the organisms. For preparation of solid media by the disk diffusion method, 15 mL of sterilized nutrient agar (NA) and Sabouraub dextrose agar (SDA) for antibacterial and antifungal studies respectively were poured and solidified into each petri plate. The suspension of the test microorganisms (0.1 mL) was swabbed by a sterile glass spreader on to individual media plates. A sterile paper disk (6mm in diameter) was saturated with a solution of the test compound and placed over the media surface and the petri dishes were incubated at 37∘C. The diameter of the inhibition zone was measured after incubation for 24 h. The minimum inhibitory concentration (MIC) values of the ligand and its complexes were also determined. The MIC value is defined as the lowest concentration of compound that prevents the visible growth of bacteria after the incubation period. In the MIC method, test solutions of each compound in DMSO were prepared by serially diluting the stock solution (500 µg/mL). A set of tubes containing Mueller–Hinton broth medium, different concentration of compounds and inoculums of the microorganism (18h old culture) were incubated at 37 °C for 24 hours to determine the MIC values.

DNA cleavage experiments

Investigation of the DNA cleavage activity of the ligand and its complexes were performed by agarose gel electrophoresis using plasmid DNA of supercoiled pMalC$_2$X of *E. Coli*. Plasmid DNA was extracted using the DNA Mini Prep Extraction Kit (BIONEER, Korea) according to the manufacturer's instructions and the plasmid were kept at -40°C for the following tests. For the extraction of plasmid DNA, the LB protocol [Pepton water: 10 g/L; Yeast

extract: 5 g/L; NaCl: 10 g/L and/or Agar: 1.5%] were used for culturing TG1 strain of *E. coli* (carried pMalC₂X DNA). 30 mL of LB broth medium was prepared and autoclaved for 20 min. at 121˚C under a pressure of 15 lb. After cooling, 50 µL of Ampiciline (100ug/ul for 1 liter) and TG1 strain were inoculated and incubated at 37˚C for 24 h. After cooling, the seed culture, 50 µL of Ampiciline was added and incubated for 24 h at 37 ˚C. The fresh bacterial culture was centrifuged to obtain the Pellet. The agarose gel for electrophoresis was prepared by dissolving 500 mg of agarose in 50 mL of TAE buffer (40mM Tris base, pH 8.0; 40mM Acetic acid; 1mM EDTA) under a boiling condition. When the temperature of the solution reached 55 ˚C, 10 µL of ethidium bromide was added and poured into the gel cassette, fitted with a comb and allowed to solidify. After solidification, the comb was carefully removed. The solid gel was placed in the electrophoresis chamber flooded with a TBE buffer. The gel electrophoresis experiment was performed by incubation of the samples containing 4 µL of 5 mg per mL of each compound in DMSO and 4 µL of plasmid DNA for 2 h at 37 ˚C. After incubation, the samples were mixed with bromophenol blue dye and along with Plasmid DNA alone, the mixture of DNA and H_2O_2 and a DNA ladder were carefully loaded into wells of the instrument. Electrophoresis was performed at a constant 100 V of electricity for about 30 min. The resulting bands of electrophoresis were visualized by UV light and then photographed.

RESULTS AND DISCUSSION

The nano-structure complexes with the general formula of [MLX₂] were synthesized by reaction between the Schiff base ligand (E)-N-(4-nitrobenzylidene)-2-(2-(4-nitrophenyl)imidazolidin-1-yl) ethanamine (L) and thiocyanate and azid salts of zinc and cadmium metals under ultrasonic conditions. The Ligand and its complexes were obtained as stable powders at room temperature. The titled compounds were characterized by physical (elemental analysis, molar conductance values) and spectral (FT-IR, ¹H and ¹³C NMR and UV–Visible) data. The molar conductivity values of the complexes were obtained in 10⁻³ M DMF solutions. Low molar conductivities of them in the range 5.22-13.97 cm² Ω⁻¹M⁻¹ indicate that the complexes are non-electrolytes and stable against dissociation in DMF (Table 1) [24]. The decomposition temperatures of the titled complexes are in the range of 143-185˚C. Figure 1 illustrates the suggested structures of the free ligand and its

complexes. The experimental data are in good agreement with the suggested structures for them. The TEM images of the complexes (Figure 2) well approve their nano- structure character. TEM images analyses suggested average particle sizes of 85.11, 25.32 and 39.78 nm for zinc thiocyante, zinc azide and cadmium thiocyante complexes respectively.
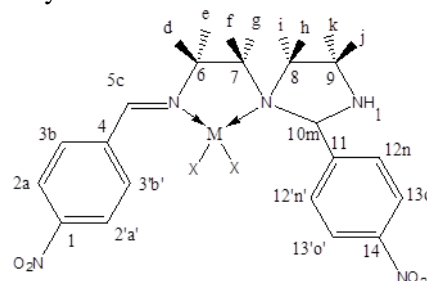

Fig. 1. Proposed structure for the azide and thiocyanate complexes with the general formula of MLX₂ wherein M= zinc(II), cadmium(II) and X= SCN⁻ and N₃⁻.
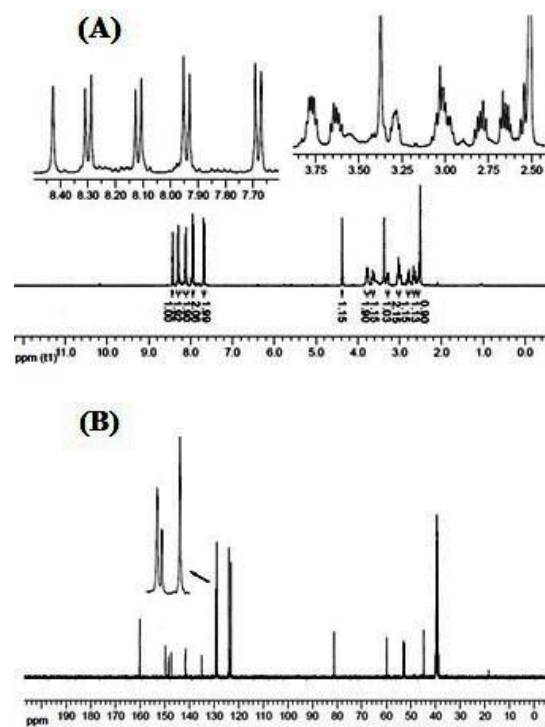

Fig. 2. ¹H NMR (A) and ¹³C NMR (B) of ZnL(NCS)₂ respectively.

Infrared and UV–Visible spectra

The characteristic IR spectral data of the complexes as compared with the ligands have been listed in Table 2. The IR spectrum of the Schiff base ligand exhibited a sharp peak at 1645 cm⁻¹ assigned to the vibration frequency of the azomethine group [25]. Appearance of the C=N vibration frequency and absence of the absorption bands of the starting materials including aldehyde

and amine at 1703 and 3100–3300 cm^{-1} provides evidence to successfully synthesis of the Schiff base ligand. The azomethine signal in the infrared spectra of all complexes shifted to the lower frequencies by 6-9 cm^{-1} toward lower energies [26-28]. The red shift of the azomethine peak indicates that the imine nitrogen atom is well bound to the central metal ions. This red shift may be due to π-back bonding of metal to ligand orbitals after coordination that reduces the bond order of the iminic bond leading to vibration at lower energies. The ligand spectrum shows a stretching vibration frequency of N-H at 3210 cm^{-1} as a broad peak due to widely internal hydrogen bonding which is observed in the complexes spectra at 3216-3268 cm^{-1} as a medium intensity band. This change in the shape and intensity of the vibration frequency of the N-H peak in the spectra is considered as confirmation of the coordination of ligand to metal ions [29]. The absorption peaks at (3101 and 3071), (2941 and 2886) and 2848 cm^{-1} are assigned to the stretching frequencies of aromatic, aliphatic and iminic CH bonds respectively. After coordination, these peaks shifted to the higher of the lower wave numbers. The stretching vibration bands of asymmetric (ν_{asym}) and symmetric (ν_{sym}) –NO$_2$ groups were observed at 1518 and 1346 cm^{-1} [30] respectively. These strong peaks shifted to another position after coordination. In the spectra of ZnL(SCN)$_2$ and ZnL(N$_3$)$_2$, the absorption peaks at 2077 and (2088 and 2063) were assigned to the coordination of SCN$^-$(N-coordination) and N$_3^-$ to zinc ions [30-34]. In the IR spectra of the cadmium thiocyanate complex, the appearance of two absorption peaks at 2089 and 2066 cm^{-1} for coordinated thiocyanate may be assigned to coordinated thiocyante in [CdL(NCS)$_2$]. Finally, the appearance of some weak absorption peaks in the range 482-495 cm^{-1} in the complexes spectra were

assigned to the M-N bond that is considered as another evidence for the synthesis of the complexes [35-37].

Electronic spectra of the ligand and its complexes were recorded in DMF at room temperature and their spectral data including the λ$_{max}$ values are listed in Table 2. A band at 278 nm attributed to the π- π* transition (iminic and benzene ring) is observed in the electronic spectra of the ligand and after formation of the complexes, this band shows a blue shift to a lower value of wavelength at 267 nm suggesting the coordination of the iminic nitrogen to the metal ions [19-23]. Other possible transitions such as the d-d transition and the metal to ligand charge transfers (MLCT) or ligand to metal charge transfers (LMCT) were not observed probably due to its overlap with the π-π* transitions of the ligand.

^{1}H and ^{13}C NMR spectra

^{1}H and ^{13}C NMR spectra were recorded at 400 MHz, using DMSO-d$_6$ solvent for the complexes and CDCl$_3$ solvent for the ligand. The signal positions observed in the complexes spectra as compared with the ligand are given in Table 3. The ^{1}H and ^{13}CNMR of the ligand and ZnL(NCS)$_2$ as typical spectra are exhibited in Figure 3. The assignments of ^{1}H and ^{13}C NMR spectral data based on Figure 1, confirm the structures of the ligand and its complexes. In the ^{1}H NMR spectrum of the ligand, the resonance of H$_m$ appeared at 4.40 ppm shifted to 4.37-4.38 ppm in the complexes spectra. In the ^{13}CNMR spectrum of the ligand, the signal at 82.37 ppm is attributed to the C$_{10}$ of the imidazolidine ring [38] that is blue shifted to 81.24-81.38 ppm in the azide and thiocyanate complexes spectra proving the coordination of the ligand with a retained structure.

Table 1. Analytical and physical data of the Schiff base ligand (L) and its azide and thiocyanate complexes.

| Run | Compound | Color | Melting point (dec.) | Yield (%) | Found (Calcd.) (%) | | | Λ$_M$ (cm^2 Ω^{-1}M^{-1}) |
					C	N	H	
1	Ligand	cream	108	65	58.3 (58.53)	18.8 (18.96)	5.1 (5.18)	5.22
2	ZnL(NCS)$_2$	cream	185	78	43.5 (43.60)	17.7 (17.85)	3.40 (3.56)	13.80
3	ZnL(N$_3$)$_2$	cream	143	72	41.5 (41.67)	29.6 (29.70)	3.8 (3.69)	6.20
4	CdL(NCS)$_2$	cream	153	80	40.2 (40.17)	16.6 (16.40)	3.4(3.20)	13.97

Table 2. Vibrational (cm^{-1}) and electronic (nm) spectral data of the Schiff base (L) and its complexes.

Compound	νNH	νCH$_{arom.}$	νCH$_{aliph}$	νCH$_{imin}$	νC=N	N (-NO$_2$)	N (-SCN)	ν(-N$_3$)	νM–N	λ$_{max}$
ZnL(NCS)$_2$	3259	3108, 3070	2929, 2881	2854	1638	1523, 1346	2077	-	482	267
ZnL(N$_3$)$_2$	3216	3108, 3062	2918	2879	1639	1525, 1342	-	2088, 2063	495	267
CdL(NCS)$_2$	3268	30104, 3064	2929	2871	1636	1528, 1344	2089, 2066	-	484	267

In the ^{1}H NMR spectrum of the ligand, the azomethine proton (H_c) is affected by complexation so that it shifts to the weaker fields from 8.33 to 8.42-8.43 ppm as a singlet indicating coordination of azomethine nitrogen to metal ions. The signals of aromatic hydrogens of free ligand were observed in the 7.69-8.30 ppm that they were found at 7.68-8.31 ppm in the azide and thiocyanate complexes spectra.

$H_{a, a'}$ protons were found as a doublet signal at 8.30 ppm due to coupling with $H_{b, b'}$ appearing at 7.88 ppm as doublet signals. In the complexes spectra, these signals appeared as doublets at similar chemical shifts or at up/downfield positions. $H_{o, o'}$ protons were observed as a doublet peak at 8.18 ppm due to coupling with $H_{n, n'}$ and appeared at 7.69 ppm. Shifts of these signals to up or downfield regions are another evidence for the coordination of the ligand. Also, the signals of ethylenic hydrogens were seen in the 2.61-3.76 ppm range as eight individual multiple peaks due to the formation of a imidazolidine ring in the structure of the free ligand while these signals are shown as several multiple signals in the range of 2.53-3.78 ppm in the complexes. The signal of H_{NH} appeared as a multiple in the range of 2.6-2.78 ppm in the spectrum of the ligand that shifts to 2.99-3.02 ppm in the complexes spectra. In the ^{13}CNMR spectrum of the ligand, the iminic carbon resonance was observed at 159.59 ppm shifts to 159.98-160.02 ppm in the complexes spectra. This difference in the location of carbon resonance for the complexes with respect to the free ligand suggests good ligation to the central metal. The resonances of the aromatic carbons appeared at 148.56 for C1 and C14, 141.44 ppm for C4 and 11, 129.98 for C12, 129.81 ppm for C12', 128.70 ppm for C3 and 3', 123.98 for C2 and 2' and 123.72 ppm for C13 and 13'.
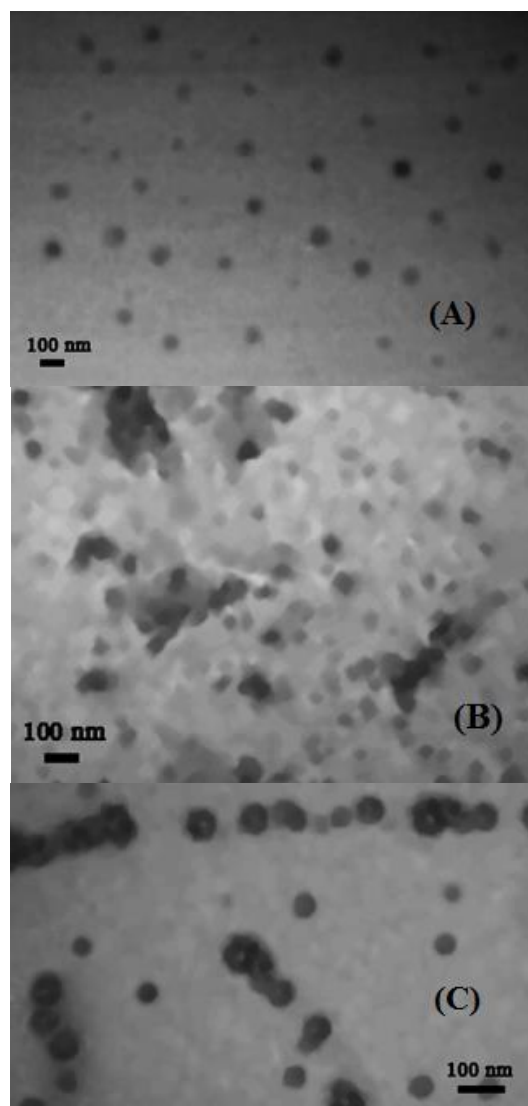

Fig. 3. TEM Images of (A) ZnL(NCS)$_2$, (B) ZnL(N$_3$)$_2$ and (C) CdL(NCS)$_2$.

Table 3.^{1}H NMR and ^{13}C NMR chemical shifts of ligand and its zinc(II), cadmium(II) complexes in ppm.

Compounds		Proposed assignment of the protons and carbons
ZnL(NCS)$_2$	^{1}H-NMR	8.42(s, 1H), 8.31(d, 2H, J= 8.80 Hz), 8.11(d, 2H, J= 8.80 Hz), 7.94(d, 2H, J= 8.80 Hz), 7.68(d, 2H, J= 8.80 Hz), 4.37(s, 1H), 3.77(m, 2H), 3.63(m, 1H), 3.29(m, 1H), 3.02(m, 2H), 2.79(m, 1H), 2.65(m, 1H), 2.54(m, 1H).
	^{13}C-NMR	160.02, 149.18, 148.44, 147.14, 141.59, 134.86, 129.19, 129.10, 128.77, 123.87, 123.09, 81.24, 59.88, 53.09, 52.70, 44.76.
ZnL(N$_3$)$_2$	^{1}H-NMR	8.43(s, 1H), 8.30(d, 2H, J= 8.80 Hz), 8.11(d, 2H, J= 8.80 Hz), 7.95(d, 2H, J= 8.80 Hz), 7.68(d, 2H, J= 8.40 Hz), 4.38(s, 1H), 3.78(m, 2H), 3.64(m, 1H), 3.26(m, 1H), 3.00(t, 2H), 2.80(m, 1H), 2.66(m, 1H), 2.53(m, 1H).
	^{13}C-NMR	160.01, 149.87, 148.44, 147.02, 141.60, 129.28, 129.09, 128.78, 123.88, 123.06, 81.32, 59.99, 53.28, 52.94, 44.73.
CdL(NCS)$_2$	^{1}H-NMR	8.43(s, 1H), 8.31(d, 2H, J= 8.80 Hz), 8.10(d, 2H, J= 8.80 Hz), 7.94(d, 2H, J= 9.20 Hz), 7.68(d, 2H, J= 8.40 Hz), 4.38(s, 1H), 3.76(m, 2H), 3.64(m, 1H), 3.24(m, 1H), 2.99(t, 2H), 2.80(m, 1H), 2.66(m, 1H), 2.53(m, 1H).
	^{13}C-NMR	159.98, 150.34, 148.44, 146.94, 141.60, 132.47, 129.04, 128.85, 128.77, 123.88, 123.03, 81.38, 60.05, 53.39, 53.09, 44.73.

After formation of complexes, these signals are shifted to down or up fields and exhibited at 149-18-150.34(C1), 148.44(C14), 146.94-147.14(C4), 141.59-141.60(C11), 129.04-129.28(C12), 128.85-129.10(C12'), 128.77-128.78(C3 and 3'), 123.87-123.88(C2 and 2') and 123.03-123.09(C13 and 13'). The ligand spectrum showed four individual peaks for C8, C6, C9 and C7 as aliphatic carbons at 61.10, 53.51, 53.46 and 45.30 ppm respectively. The coordination of the ligand with the metal ions leads to changes in their chemical shifts so that they appeared at 57.60-60.05 ppm for C8, 53.09-53.28 ppm for C6, 52.70-53.09 ppm for C9 and 44.60-44.73 ppm for C7 in the spectra of all complexes. In the spectrum of $ZnL(NCS)_2$ and $[CdL(SCN)_2]$, the signal of the carbon resonance of –SCN anions appeared at 134.86 and 132.47 ppm respectively [19-23]. Finally it is obvious that the resultant data obtained from the ^1H and ^{13}CNMR spectra well confirms the suggested structure of the complexes as shown in Figure 1.

Thermal analysis

Thermogravimetric and differential thermogravimetric analysis (TG/DTG) of the complexes were studied under an N_2 atmosphere from room temperature to 900 ℃ (Fig. 4). Thermal studies of the solid complexes were performed to show more insight into the structure of the reported complexes. The thermal analyses of the data including the temperature range, the mass loss (%) and the thermodynamic activation parameters of the decomposition steps of the complexes are listed in Table 4. The decomposition of $ZnL(NCS)_2$ occurred in six successive thermal steps and in the final step, the percentage of mass lose was 69.78%. It seems that the thiocyanate groups and the organic segment are eliminated respectively. A limited amount of zinc-organic compound is left at the final step. Major mass lose of $ZnL(NCS)_2$ occurred at 510-680 ℃ with a weight loss of 41.93%. The TG plots of $ZnL(N_3)_2$ and $CdL(NCS)_2$ showed three successive thermal degradation steps and the total mass loss(%) at the end of the thermal decomposition was 82.03% and 61.47% and the major decomposition occurred at the third thermal step 390-900 ℃ and 430-600 ℃ respectively. Likewise in these complexes, azide and thiocyanate as well as organic parts are the major lost segments such that zinc and cadmium metals are major residuals at the final step. The thermodynamic activation parameters of the decomposition processes of the complexes including the Arrhenius constant (A), the activation energy (E*), enthalpy (ΔH*), entropy (ΔS*) and Gibbs free energy of

decomposition (ΔG*) were evaluated based on plots using the Coats– Redfern relation [39-41].

The Coats-Redfern equation for the first order process is in the form:

$$\log[\log\{W_f/(W_f - W)\}/T^2] = \log[AR/\Theta E^*(1 - 2RT/E^*)] - (E^*/2.303RT) \quad \text{(Eq. 1)}$$

Where W_f is the mass loss at the completion of the reaction, W is the mass loss up to temperature T; ($W_r = W_f - W$), R is the gas constant, E^* is the activation energy in J mol^{-1}, Θ is the heating rate. Since $1-2RT/E^*1$, a plot *vs.* $1/T$ was drawn and E^* was calculated from the slope and the A (Arrhenius constant) was found from the intercept. Fig. 5 shows the plots of three steps of decomposition for $CdL(NCS)_2$.
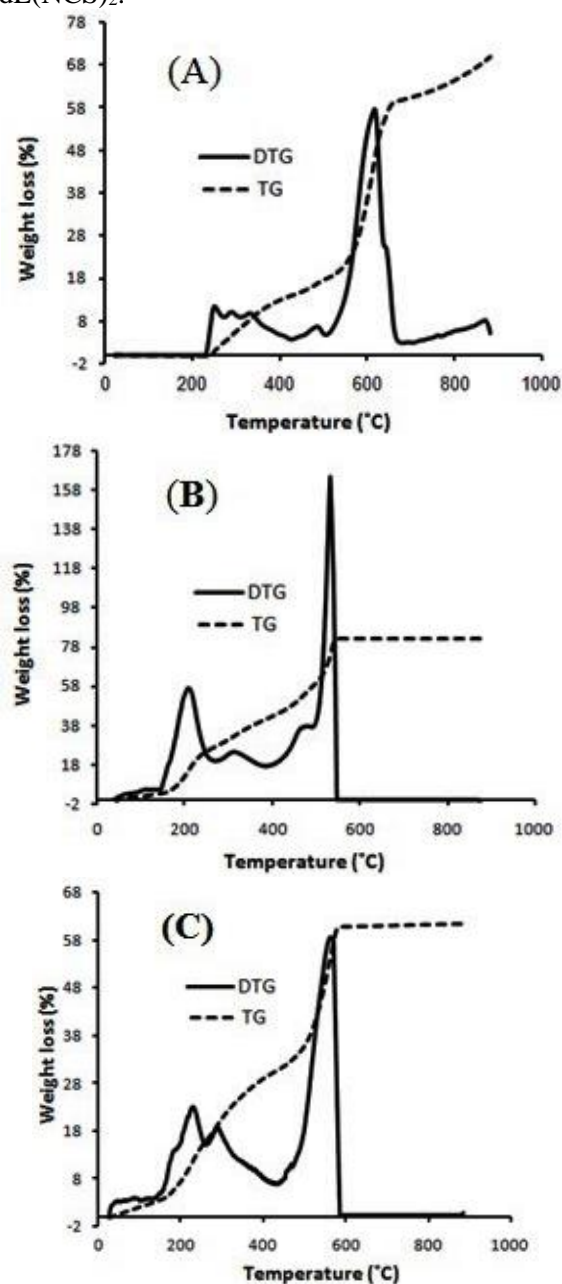

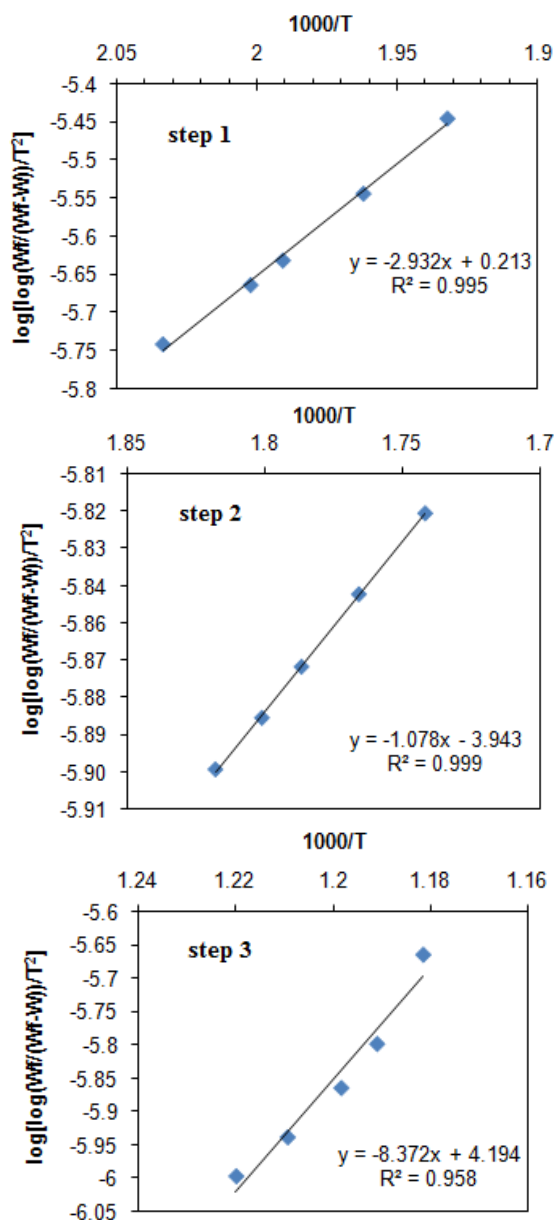**Fig. 4.** TG diagrams of the $ZnL(SCN)_2$ complex(A), $ZnL(N_3)_2$ complex(B) and $CdL(NCS)_2$complex (C).

214

step 1

$y = -2.932x + 0.213$
$R^2 = 0.995$

step 2

$y = -1.078x - 3.943$
$R^2 = 0.999$

step 3

$y = -8.372x + 4.194$
$R^2 = 0.958$

Fig. 5. Coats-Redfern plots of the three decomposition steps of $CdL(NCS)_2$ complex.

The equations used to calculate the activation entropy ΔS^*, the activation enthalpy ΔH^* and the free energy of activation ΔG^* are:

$$\Delta S^* = 2.303[log(Ah/kT)R] \qquad (Eq. 2)$$
$$\Delta H^* = E^* - RT \qquad (Eq. 3)$$
$$\Delta G^* = \Delta H^* - T\Delta S^* \qquad (Eq. 4)$$

where k and h are the Boltzmann and Planck constants respectively.

The resultant data listed in table 4 is found in the range 20.64-422.96 k J mol⁻¹ for energies (E^*) at different steps of thermal decomposition indicating relative thermal stability for the complexes. Except for two steps, the entropy of activation (ΔS^*) is negative and the value of ΔS^* is recorded in the range -271-509 kJ mol-1. As reported in the literature, the negative values suggest an associated

mechanism at the rate determining step of thermal degradation. On the other hand the negative values may be due to a lower rate of thermal decomposition than the normal decomposition process [39, 40]. The values of ΔH^* and ΔG^* are evaluated in the range 16.055 - 418.591 kJ.mol⁻¹ and 138 - 330 kJ.mol⁻¹ respectively. The positive values for ΔH^* and ΔG^* at all steps indicate the endothermic character of thermal decomposition for these compounds.

Antibacterial and antifungal activity

The biological activities of the complexes as compared with the ligand were investigated by two methods containing disk diffusion and minimum inhibitory concentration (MIC) techniques against *Escherichia coli* and *Pseudomonas aeruginosa* as Gram negative; *Staphylococcus aureus* and *Bacillus subtillis* as Gram positive and *Candid albicans* as a fungus. The experimental results have been tabulated as Table 5. All tested compounds showed a notable antimicrobial activity. Comparing the biological activity of the Schiff base ligand with respect to its complexes showed that metal complexes potentially have more antibacterial and anti-fungal activity against the microorganisms as mentioned above. In general, the metal complexes are more active than the ligands because metal complexes may serve as a vehicle for activation of the ligand as the principle cytotoxic species [42]. According to Overtone's concept and Tweedy's chelation theory [43, 44], the overlap of the ligand orbitals and metal ion valence orbitals leads to π-electron delocalization in the ligand and considerably reduces the polarity of the metal ion and therefore increases the lipophilic character of the compound that causes more diffusion into the cell membranes. In this way, the growth of bacteria and/or fungi can be disturbed by blocking the metal coordination sites of the bacteria and/or fungi enzymes. The MIC method was also carried out for all the compounds using 15.63, 31.25, 62.50, 125, 250, 500 µg/mL concentrations. The MIC value of the ligand for all bacteria is 500 µg/mL. After coordination of the ligand to metal ions, the most efficient value was found for $CdL(NCS)_2$ (125 µg/mL) with respect to *Staphylococcus aureus* as Gram positive bacteria. In the disk diffusion method, the diameter zone of the inhibitory effect was recorded in millimeters. For all complexes against all microorganisms, this value was more than the parent Schiff base ligand.

Table 4. Thermal analysis data including the temperature range, mass loss(%) and thermodynamic activation parameters of the decomposition steps of the complexes

Compound	Temperature step(°C)	~Mass loss(%)	Total Mass massloss(%)	E^*(kJmol^{-1})	A(s^{-1})	ΔS^*(kJmol^{-1})	ΔH^*(kJmol^{-1})	ΔG^*(kJmol^{-1})
ZnL(NCS)$_2$	230-275	2.92	69.78	422.96	3.96×10^{39}	5.09×10^2	418.591	1.51×10^2
	275-315	3.47		102.265	1.07×10^7	-1.16×10^2	97.577	1.63×10^2
	315-430	7.47		46.413	1.25×10^1	-2.30×10^2	41.368	1.81×10^2
	430-510	3.87		89.532	6.33×10^3	-1.80×10^2	83.214	2.20×10^2
	510-680	41.93		167.729	2.00×10^7	-1.14×10^2	160.318	2.62×10^2
	680-900	10.12		228.425	2.01×10^8	-9.72×10^1	218.921	3.30×10^2
ZnL(N$_3$)$_2$	120-270	27.07	82.03	60.477	7.61×10^3	-1.75×10^2	56.520	1.39×10^2
	270-385	13.85		20.641	1.03×10^{-1}	-2.69×10^2	16.055	1.64×10^2
	390-900	41.11		226.319	4.06×10^{12}	-1.03×10^1	220.748	2.28×10^2
CdL(NCS)$_2$	120-260	15.87	61.47	56.139	2.14×10^3	-1.85×10^2	52.192	1.40×10^2
	260-430	14.77		20.641	8.49×10^{-2}	-2.71×10^2	16.055	1.65×10^2
	430-600	30.19		160.300	5.40×10^7	-1.04×10^2	154.728	2.24×10^2

Table 5. Antibacterial and antifungal activities of 25 µg/disks of the Schiff based ligand and its complexes based on the zone of inhibition, the growth of microorganisms(mm) and MIC(µg/mL).

Compound	Gram negative bactria				Gram positive bacteria				Candida albicans
	Escherichia coli		Pseudomonas aereuguinosa		Bacillus subtillis		Staphylococcus aureus		
	MIC (µg/mL)	zone (mm)	MIC (µg/mL)	zone (mm)	MIC (µg/mL)	zone (mm)	MIC (µg/mL)	zone (mm)	zone (mm)
Ligand	500	11.50	500	6.80	500	14.46	500	10.00	17.40
ZnL(NCS)$_2$	250	15.50	500	8.44	250	17.00	250	12.00	24.80
ZnL(N$_3$)$_2$	500	12.20	500	7.90	500	15.00	500	11.50	21.80
CdL(NCS)$_2$	250	15.20	500	8.60	500	14.80	125	16.20	18.50

As seen in Table 5, all compounds have the lowest inhibition effect with respect to *Pseudomonas aereuguinosa* among tested bacteria.

The bioassay data for ligands showed maximum and minimum efficiency with respect to *Bacillus subtillis* with inhibition zone of 14.46 mm and *Pseudomonas aereuguinosa* with inhibition zone of 6.80 mm respectively. A comparable investigation between all the complexes indicated that the growth of bacteria is more inhibited by ZnL(NCS)$_2$ for *Escherichia coli* and *Bacillus subtillis*. CdL(NCS)$_2$ efficiently stopped the growth of *Pseudomonas aereuguinosa* and *Staphylococcus aureus*. The growth inhibition effects of the ligand and its complexes with respect to *Candida albicans*as, as a fungus, were studied and ZnL(NCS)$_2$ with inhibition zone of 24.80 mm was selected as an efficient antifungal as compared with the free ligand.

DNA cleavage efficiency

The DNA cleavage ability of the complexes as compared with the free ligand was monitored by the agarose gel electrophoresis method with respect to pMalC$_2$X DNA of *E. Coli*. Three forms of DNA containing a supercoiled form (Form I), open circular (nicked) form (Form II) and the linear form (Form III) were separated based on the difference in the rate of migration by electrophoresis. When the original supercoiled form (Form I) of plasmid DNA is nicked, an open circular relaxed form (Form II) will be exist in the system and the linear form (Form III) can be found upon further cleavage. The compact Form I migrates relatively faster while the nicked Form II migrates slowly, and the linearized form (Form III) migrates between Forms I and II. The nuclease activity of the complexes as compared with the free ligand have been assessed by their ability to convert supercoiled pMalC$_2$X DNA from Form I to Form II and Form III. All the metal complexes and free ligands were able to convert supercoiled DNA into an open circular and linear form of DNA. These changes were illustrated in gel electrophoresis by the intensity of the bands. The results of DNA cleavage are given in Figure 5. In this figure L, X and C are attributed to the ladder, mixture of DNA , H$_2$O$_2$ and control DNA respectively. The lanes 1 to 4 are attributed to mixtures of DNA with a ligand,

$ZnL(NCS)_2$, $ZnL(N_3)_2$ and $CdL(NCS)_2$ respectively.

The effect of the compounds in cleavage of the suppercoiled DNA to the form II and III is determined by diminishing in intensity of the band of the suppercoiled $pMalC_2X$ DNA. It seems that $ZnL(NCS)_2$ and $CdL(NCS)_2$ are more efficient for the cleavage of the supper coiled form to the linear form of DNA as compared with the other tested compounds. The DNA cleavage ability of the complexes may depend on the binding of the DNA molecule to the metal complexes. However, the nature of the reactive intermediates involved in the DNA cleavage by the complexes is not clear. According to the experimental data from the DNA cleavage studies, it may be correct to say that the cleavage of genome is responsible for the death of some of the studied microorganisms [45].
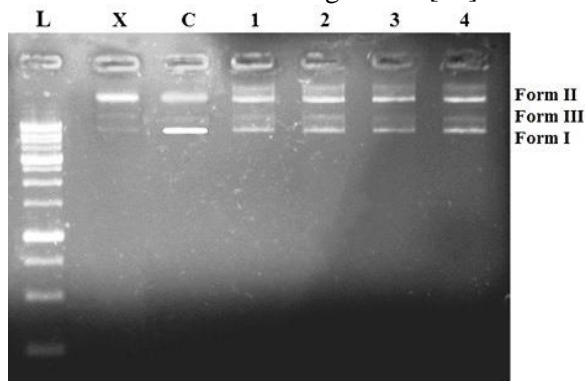

Fig. 6. Gel electrophoresis diagram for DNA cleavage activity of ligand and its complexes. lane L: ladder, lane X: DNA + H_2O_2; lane C: control DNA, lanes 1 to 4: ligand, $ZnL(NCS)_2$, $ZnL(N_3)_2$ and $CdL(NCS)_2$ respectively.

CONCLUSION

In this research three new azide and thiocyanate complexes of an imidazolidine Schiff base ligand were synthesized and characterized by spectral (IR, UV–Visible, ^1H and ^{13}C NMR) and physical techniques. The observable changes in IR and NMR spectra in the complexes with respect to the free ligand well suggest the formation of the mentioned complexes. IR peaks appeared for azide and thiocyanate well confirm the coordination of these anions to metal centers in the inner coordination sphere. The spectral data suggest the formula structure of MLX_2 for the complexes. The nano-size character of the synthesized complexes was confirmed by the TEM images. Moreover the thermal behavior of the complexes was studied by their thermal analysis and then some activation thermodynamic parameters such as A, E*, ΔH*, ΔS* and ΔG* were calculated based on the thermal analysis plots of TG/DTG. The antimicrobial

behaviors of the complexes against the *Escherichia coli*, *Pseudomonas aereuguinosa*, *Staphylococcus aureus* and *Bacillus subtillis* and a fungus entitled as *Candida albicans* were investigated. Finally, the DNA interaction of the compounds with $pMalC_2X$ DNA of *Escherichia coli* was investigated and it was revealed that $ZnL(NCS)_2$ and $CdL(NCS)_2$ are more successful for the cleavage of DNA that other compounds.

REFERENCES:

1. A.K. Sharma, S. Chandra, *Spectrochim.Acta A,* **78**, 337 (2011).
2. P.M. Vimal Kumar, P.K. Radhakrishnan, *Inorg.Chim.Acta,* **375**, 84 (2011).
3. 3.M. Sutradhar, T.R. Barman, M.G.B. Drew, E. Rentschler, *J.Mol.Struct.,* **1041**, 44 (2013).
4. B. Gao, M. Wan, J. Men, Y. Zhang, *Appl.Catal. A: General,* **10**,156 (2012).
5. M. H. Habibi, E. Shojaee, G. S. Nichol, *Spectrochim. Acta A,* **98**, 396 (2012).
6. B. P. Baranwal, K Tripathi, A. K. Singh, S. Tripathi, *Spectrochim. Acta A,* **91**, 365 (2012).
7. S. Ershad, L. Sagathforoush, G. Karim-nezhad, S. Kangari, *Int. J. Electrochem. Sci.,* **4**, 846 (2009).
8. G. Grivani, G. Bruno, H.A. Rudbari, A.D. Khalaji, PegahPourteimouri, *Inorg. Chem. Commun.,* **18**, 15 (2012).
9. J. Li, J. Hu, Y. Gu, F. Mei, T. Li, G. Li, *J. Mol. Catal. A: Chem.*, **340**, 53 (2011).
10. W. Zeng, J. Li, S. Qin, *Inorg.Chem.Commun.,* **9**, 10 (2006).
11. M. M. Tamizh, R. Karvembu, *Inorg. Chem. Commun.,* **25**, 30 (2012).
12. D. Arish, M. Sivasankaran Nair, *Spectrochim.Acta A,* **82**, 191 (2011).
13. G. Hu, G. Wang, N. Duan, X. Wen, T. Cao, S. Xie, W. Huang, *ActaPharma.Sin.B,* **2**, 312 (2012).
14. S. Sathiyaraj, K. Sampath, R.J. Butcher, R. Pallepogu, C. Jayabalakrishnan, *Eur. J. Med. Chem.,* **64**, 81 (2013).
15. S. Akine, T. Taniguchi, W. Dong, S. Masubuchi, T. Nabeshima, *J. Org. Chem.*, **70**, 1704 (2005).
16. W. K. Dong, Y. X. Sun, Y. P. Zhang, L. Li, X. N. He, X. L. Tong, *Inorg.Chim.Acta,* **362**, 117 (2009).
17. M. F. Summers, L.G. Marzilli, N. Bresciani-Pahor, L. Randaccio, *J. Am. Chem. Soc.*, **106**, 4478 (1984).
18. A. K. Singh, O. P. Pandey, S. K. Sengupta, *Spectrochim. Acta A,* **85**, 1 (2012).
19. M. Daszkiewicz, *CrystEngComm*, **15**, 10427 (2013).
20. M. Montazerozohori, S. Zahedi, A. Naghiha, M. Montazer Zohour, *Mater. Sci. Eng. C,* **35**, 195 (2014).
21. M. Montazerozohori, S. Zahedi, M. Nasr-Esfahani, A. Naghiha, *J. Ind. Eng. Chem.*, **20**, 2463 (2014).
22. M. Montazerozohori, S.A. Musavi, A. Naghiha, M. Montazer Zohour, *Spectrochim. Acta A*, **129,** 382 (2014).

23. M. Montazerozohori, S.A. Musavi, A. Naghiha, S. Veyseh, *J. Chem. Sci.*, **126**, 227(2014).
24. Y. Harinath, D. H. K. Reddy, B. N. Kumar, Ch. Apparao, K. Seshaiah, *Spectrochim. Acta A,* **101**, 264 (2013).
25. A. DehnoKhalaji, G. Grivani, M. Seyyedi, K. Fejfarovac, M. Dusek, *Polyhedron,* **49**, 19 (2013).
26. M. Shebl, *Spectrochim.Acta A,* **73**, 313 (2009).
27. A. DehnoKhalaji, G. Grivani, M. Rezaei, K. Fejfarovac, M. Dusek, *Polyhedron*, **30**, 2790 (2011).
28. S. Chandra, S. Bargujar, R. Nirwal, N. Yadav, *Spectrochim.Acta A,* **106**, 91 (2013).
29. B. Dede, F. Karipcin, M. Cengiz, *J. Hazard. Mater.,* **163**, 1148 (2009).
30. M. Montazerozohori, S.A. Musavi, *J. Coord. Chem.,* **61**, 3934 (2008).
31. B. Samanta, J. Chakraborty, C.R. Choudhury, S.K. Dey, D.K. Dey, S.R. Batten, P. Jensen, G.P.A. Yap, S. Mitra. *Struct.Chem.,* **18**, 33 (2007).
32. C. Zhang, G. Tian, B. Liu. *Transition Met. Chem.,* **25**, 377 (2000).
33. S. Sen, P. Talukder, G. Rosair, S. Mitra. *Struct.Chem.,* **16**, 605 (2005).
34. N.A. Illan-Cabeza, F. Hueso-Urena, M.N. Moreno-Carretero, J.M. Martınez-Martos, M.J. Ramırez-Exposito, *J. Inorg. Biochem.,* **102**, 647 (2008).
35. L.P. Nitha a, R. Aswathy a, Niecy Elsa Mathews a, B. Sindhukumari b, K. Mohanan, *Spectrochim.Acta A,* **118**, 154 (2014).
36. G. Grivani, V. Tahmasebi, K. Eskandari, A. DehnoKhalaji, G. Bruno, H. AmiriRudbari, *J. Mol. Struct.,* **100**,1054 (2013).
37. Y. Harinath, D. H. K. Reddy, B. N. Kumar, Ch. Apparao, K. Seshaiah, *Spectrochim. Acta A,* **101**, 264 (2013).
38. F. Yue, L. Gang, T. Xiu-Mei, W. Ji-De, W. Wei, *Chin. J. Struct. Chem.,* **27**, 455 (2008).
39. A. A. Soliman, *J. Therm. Anal.Calorim.,* **63,** 221 (2001).
40. R.R. Zaky, T.A. Yousef, K.M. Ibrahim, *Spectrochim. Acta A,* **97**, 683 (2012).
41. S. Sen, P. Talukder, G. Rosair, S. Mitra, *Struct Chem.,* **16**, 605 (2005).
42. D.H. Petering, H. Sigel, Metal Ions in Biological Systems, vol. 2, Marcel Dekker, New York,1973, p. 167.
43. B.G. Tweedy, Phytopathalogy, **55,** 910 (1964).
44. J.W. Searl, R.C. Smith, S.J. Wyard, *Proc. Phys. Soc.,* **78,** 1174 (1961).
45. A. Kulkarni, S.A. Patil, P.S. Badami, *Eur. J. Med. Chem.*, **44**, 2904 (2009).

НАНО-СТРУКТУРИРАНИ ЦИНКОВ И КАДМИЕВ АЗИД И ТИОЦИАНАТНИ КОМПЛЕКСИ: СИНТЕЗА, ХАРАКТЕРИЗИРАНЕ, ТЕРМИЧНИ, АНТИМИКРОБНИ И ДНК-ВЗАИМОДЕЙСТВИЯ

С. А. Мусави[1],М. Монтазерозохори[1]*, М. Наср-Есфахани[1], Р. Нагиха[2], М.Монтазер Зохоур[3]

[1]*Департамент по химия, Университет Ясудж, Ясудж 75918-74831, Иран*
[2]*Департамент по зоология, Земеделски факултет, Университет Ясудж, Ясудж, Иран.*
[3]*Изследователски център по генетика на неинфекциозните заболявания, Медицински университет в Захедан, Иран*

(Резюме)

Приготвени са три нано-структурирани азиди и тиоцианати на цинка и кадмия и техни комплекси с бази на Schiff като лиганди, Те са охарактеризирани чрез измервания на проводимостта, елементен анализ, IR, UV–Visible, 1H и 13C ЯМР-спектроскопия и термо-гравиметрични изследвания. Забележимите промени в спектралните данни предполагат координиране на лигандите към цинковия и кадмиевия атом. Предлага се следната емпирична формула на комплексите: MLX2. Нано-размерната структура на комплеските се потвърждава чрез трансмисионна електронна микроскопия (ТЕМ). Средният размер на комплексите е определен в интервала на 25.32 - 85.11 nm. Резултатите от термичния анализ показват, че цинковият изоцианат се разпада на шест последователни стъпки, докато кадмиевите комплекси се разлагат на три етапа. От термогравиметричните криви и от диференциално-термогравиметричния анализ са определени термодинамични параметри, като активиращата енергия, енталпията, ентропията, свободната енергия на активация по Гибс, както и константата на Арениус. Изследвана е антимикробната активност спрямо бактериите *Escherichia coli, Pseudomonas aereuguinosa, Staphylococcus aureus, Bacillus subtillis* и гъбичките *Candida albicans*. ZnL(NCS)2 има най-висока анти-гъбична активност спрямо *Candida albicans* сравнение с останалите комплекси. Накрая е изпитано взаимодействието на комплексите с ДНК (pMalC2X DNA от *Escherichia coli*) за да се изследва потенциала на разкъсване.